

Structure and magnetism of ultrathin Co film grown on Pt(100)

Minghu Pan, Ke He, Lijuan Zhang, Jinfen Jia, and Qikun Xue

State Key Laboratory for Surface Physics and International Center for Quantum Structures, Institute of Physics, Chinese Academy of Sciences, Beijing 100080, China

Wondong Kim^{a)} and Z. Q. Qiu^{b)}

Department of Physics, University of California at Berkeley, Berkeley, California 94720

(Received 30 September 2004; accepted 8 February 2005; published 24 June 2005)

Ultrathin Co films were deposited on Pt(100) at room temperature in ultrahigh vacuum, and investigated *in situ* by low-energy electron diffraction, scanning tunneling microscopy (STM), and surface magneto-optic Kerr effect. The Co film was grown into a wedge shape to provide a continuous change of the film thickness. We find that the Co film forms single-crystal ultrathin films at least up to 5 monolayers (ML). For as-grown films, we observe only in-plane magnetization. After annealing the film, the Co film develops a perpendicular magnetic anisotropy, leading to a spin reorientation transition at 2.7 ML Co thickness. STM measurements were performed at room temperature both before and after annealing the film. We found very different surface morphology and alloy formation after the film annealing, and attribute the perpendicular magnetic anisotropy to the formation of the Co-Pt alloy layer at the Co/Pt(100) interface. © 2005 American Vacuum Society. [DOI: 10.1116/1.1885025]

I. INTRODUCTION

Pd and Pt exhibit many similar properties as substrates for the study of ultrathin films. In particular, ferromagnetic thin films grown on Pt or Pd substrate attract great attention in magnetic nanostructure research. Many interesting phenomena have been observed in this system, such as the enhanced magneto-optic effect,^{1,2} induced magnetic moment,^{3,4} and the extraordinary Hall effect,⁵ etc. Co/Pt and Co/Pd were also applied recently to study other phenomena, such as exchange bias⁶ and oscillatory magnetic interlayer coupling.⁷ Among all these discoveries, the presence of perpendicular magnetization has in particular promoted many research activities on topics of the magnetic anisotropy,^{8,9} spin reorientation transition,¹⁰ magnetic domains,^{11,12} the modification of the magnetic properties by chemical absorption and covering layer,^{13–15} etc. For the Co/Pd system, experiments show that all three (100), (110), and (111) surfaces exhibit perpendicular magnetic surface anisotropy whose magnitude is independent of the crystal orientation.⁸ The similarity of Pd and Pt makes it possible to search for the perpendicular magnetic anisotropy of Co/Pt systems in (100), (110), and (111) orientations. The experimental results, however, show that the Co/Pt system behaves very differently from the Co/Pd system. For example, while Co films grown on Pt(111) substrate exhibit perpendicular magnetization below a critical thickness,¹⁶ Co film grown on Pt(100) has in-plane magnetization.¹⁷ Detailed structural characterizations reveal that the variation of the magnetic anisotropy for different Co/Pt surface orientations is probably related to the different interfacial properties.¹⁸ In fact, the dependence of the easy magnetization axis on the growth condition was reported in a

similar system: Fe/Pd(100). It was shown that the Fe/Pd(100) system has an in-plane magnetization for room-temperature-grown Fe film and a perpendicular magnetization for low-temperature-grown Fe film.¹⁹ Structural characterization indeed confirms that the initial growth of Fe on Pd(100) exhibits very different growth regimes on substrates at low and room temperature.^{20,21} The interesting question is why Co/Pt(100) does not carry a perpendicular magnetic anisotropy, while Co/Pt(111), Co/Pd(111), and Co/Pd(100) all possess perpendicular magnetization. Is this because Co/Pt(100) has a very different interfacial property or because the “correct” growth condition has not yet been achieved? To elucidate the magnetic anisotropy of magnetic thin films on Pd and Pt substrates, it becomes very important to verify if a perpendicular magnetization can be established in the Co/Pt(100) system under a special condition. In this article, we report the observance of perpendicular magnetic anisotropy in the Co/Pt(100) system. We show that room-temperature-grown Co/Pt(100) has an in-plane magnetization, but annealing the film at 400 °C leads to a perpendicular magnetic anisotropy.

II. EXPERIMENT

The experiments are performed in an Omicron ultrahigh vacuum system (8×10^{-11} mbar base pressure) equipped with low-energy electron diffraction (LEED), scanning tunneling microscopy (STM), and surface magneto-optic Kerr effect (SMOKE). A Pt(100) single crystal 1 cm in diameter and 1 mm thick is cleaned with a combination of Ar-ion sputtering at 1 keV and annealing at 700–900 °C. The cleaning process continues until LEED shows the well-known Pt(100) reconstruction pattern.²² Co films are grown on the Pt(100) substrate at room temperature by dc heating of a tungsten filament that is precoated with Co using electrodeposition. The Co films are grown either into a uniform

^{a)}Also at Korea Research Institute of Standards and Science, Yuseong, Daejeon 305-600, Republic of Korea

^{b)}Electronic mail: qiu@socrates.berkeley.edu

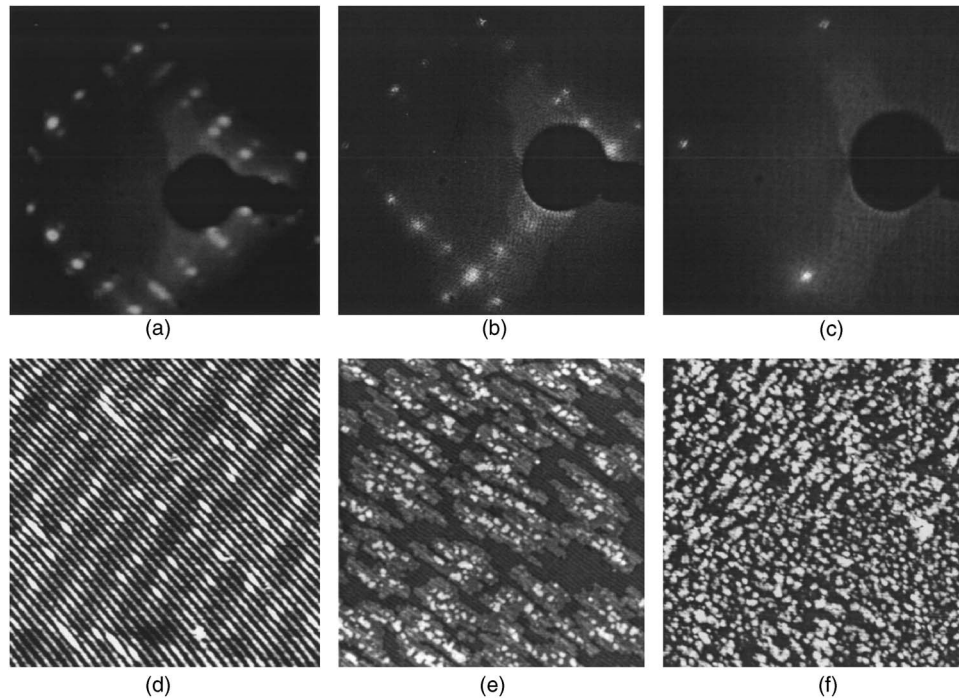


FIG. 1. LEED and STM results of Pt(100) [(a) and (d)], Co(0.6 ML)/Pt(100) [(b) and (e)], and Co(2.0 ML)/Pt(100) [(c) and (f)] for as-grown films. The STM image size is $50 \text{ nm} \times 50 \text{ nm}$ for Pt(001) and $100 \text{ nm} \times 100 \text{ nm}$ for Co/Pt(100).

thickness film or into a wedge shape to facilitate a continuous change of the film thickness. The wedge is made by translating the Pt(100) substrate behind a knife-edge shutter during the Co film growth. After finishing the film growth, the sample is characterized *in situ* by Auger electron spectroscopy, LEED, and STM. All STM images reported here are recorded at room temperature with a tunneling current of 20 to 50 pA.

SMOKE measurements are performed *in situ* at room temperature. Two pairs of electromagnets supply a magnetic field either parallel or perpendicular to the film surface to permit the longitudinal and polar SMOKE measurements without the need to move the sample position. An intensity-stabilized He-Ne laser serves as the SMOKE light source. The incident beam is linearly polarized either in the *s*- or *p*-polarization mode and the incident angle is fixed at 45° relative to the normal direction of the film surface. After reflection, the beam intensity is measured by a photodiode behind a linear polarizer that is set at 1° from extinction. A quarter-wave plate is placed in the pathway of the reflection beam to eliminate the birefringence of the UHV viewport. Because the quarter-wave plate introduces a 90° phase shift between the *s* and *p* components, the measured Kerr intensity is proportional to the Kerr ellipticity.²³

III. RESULTS AND DISCUSSION

A. Structural characterization

It is well known that a clean Pt(100) surface is reconstructed and is usually referred to Pt(100)-hex-R 0.7° . This reconstruction consists of a topmost quasi-hexagonal layer that is highly anisotropic, with six-atom-wide channels run-

ning along the $[011]$ or $[01\bar{1}]$ direction.²⁴ The reconstructed Pt(100)-hex-R 0.7° surface is very sensitive to impurity. A tiny amount of residual gas such as carbon monoxide could easily convert the reconstruction to an unconstructed 1×1 Pt(100) surface.²⁵ The well characterized LEED reconstruction pattern and the STM image in our experiment [Fig. 1(a)] show that we have a clean reconstructed Pt(100)-hex-R 0.7° surface. Indeed, STM measurement [Fig. 1(d)] reveals the surface reconstruction being six-atom-wide channels running along the $[011]$ or $[01\bar{1}]$ direction. After the characterization of the Pt(100) surface, we performed LEED and STM studies of the Co/Pt(100) system. In the thickness range of 0–4 monolayer (ML) Co films on Pt(100), sharp LEED spots are always obtained, indicating the formation of single-crystal fcc Co films. However, the LEED patterns show different characteristics for Co films below and above ~ 1 ML. Figures 1(b) and 1(c) show representative LEED pictures of the Co films at 0.6 and 2.0 ML. Below ~ 1 ML Co thickness, the reconstruction LEED pattern persists with the same character as that of Pt(100) [Fig. 1(b)]. STM measurement [Fig. 1(e)] on the 0.6 ML Co film shows that most of the Co atoms form 1 ML high islands with a small portion Co forming 2 ML high islands. The unfilled Pt region has the same surface reconstruction as that of the Pt(100)-hex-R 0.7° surface. The 1 ML high islands are mixed of unconstructed and reconstructed surface. The small portion of the 2 ML high islands do not have the reconstructed surface within our STM resolution. It was shown that Pt(100) quasi-hexagonal surface plane contains 20% to 25% more Pt atoms than the 1×1 Pt(100) surface plane, and that these extra surface atoms could become adatoms to coalesce into islands and steps.

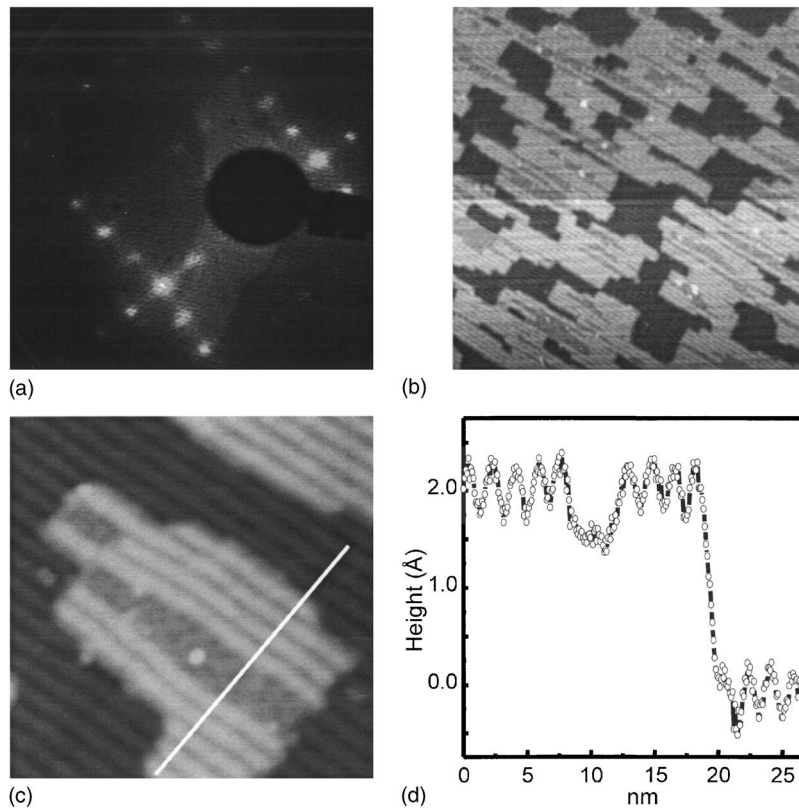


Fig. 2. LEED and STM ($100\text{ nm} \times 100\text{ nm}$) results of Co(0.6 ML)/Pt(100) [(a) and (b)] after annealing at $400\text{ }^\circ\text{C}$. (c) Close-up STM image ($30\text{ nm} \times 30\text{ nm}$) of a 1 ML high island. (d) A line scan across the island.

Photoemission experiment shows that Co adatoms grown at room temperature intermix with the Pt atoms.¹⁷ Therefore, the observed reconstructed part of the monolayer islands may result from Co-Pt intermixing. We will see this more clearly from the annealing experiment. Nevertheless, the LEED and STM results for the room-temperature-grown Co/Pt(100) suggest that the Co coverage has a tendency to remove the surface reconstruction. Indeed the reconstruction LEED pattern completely disappears once the Co film reaches 2 ML thick [Fig. 2(c)]. STM measurement shows that the 2 ML Co film consists of completely filled 1 ML layer plus small sized 2 ML and 3 ML islands. This bilayer surface roughness persists up to 4 ML thick Co film. The STM result shows that the room-temperature-grown Co film does not have an ideal layer-by-layer growth nature beyond 1 ML thickness, although the LEED result indicates the formation of single-crystal fcc film. The bilayer surface roughness is probably caused by the lattice mismatch and intermixing between the Co and Pt atoms.

After annealing the room-temperature-grown Co film at $400\text{ }^\circ\text{C}$, the contrast of the LEED spots to the background improves slightly. The LEED pattern remains as a quasi-hexagonal reconstruction below 1 ML and develops to a sharp 1×1 LEED pattern above 2 ML. The STM measurement result shows that the film morphology is very different after annealing. Below 1 ML, the film consists of 1 ML high islands with virtually no second layer present, showing that the annealing improves the surface smoothness [Figs. 2(a) and

2(b)]. In addition, most 1 ML islands exhibit the reconstruction after the annealing [Fig. 2(b)]. Figures 2(c) and 2(d) show a close-up STM image of a 1 ML island and a line scan across the island. It is clearly seen that the island consists of a reconstructed surface plus an unreconstructed area (in the middle of the island). The line scan shows that the unreconstructed area has a height less than the average height of the reconstructed island. Given the fact that the 1 ML island consists of more reconstructed area after annealing and that the Pt has a greater atomic size than the Co atom, we conclude that the reconstructed 1 ML islands are from Co-Pt alloy due to intermixing. For Co film thicker than 2 ML, the surface reconstruction is no longer present, as indicated by both LEED and STM measurements. We do not know the amount of Co-Pt intermixing in the second layer, but the absence of the reconstruction for the second layer surface indicates that the Co-Pt intermixing in the second layer should be less than that of the first Co layer. The diffusion of Co atoms into Pt was also reported in the (111) surface,²⁶ and under certain conditions ordered alloy was formed. Although our STM measurement cannot resolve the Co and Pt atoms, it is unlikely that Co/Pt(100) forms an ordered alloy layer because no corresponding LEED spots were observed.

B. Magnetic properties

The magnetic ordering of Co/Pt(100) films grown at room temperature was measured by *in situ* SMOKE. In the

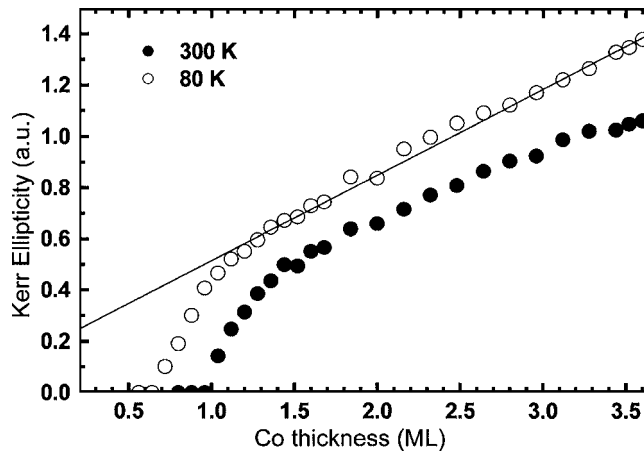


FIG. 3. Longitudinal Kerr remanences of as-grown Co/Pt(100) films measured at 300 K (filled circles) and 80 K (hollow circles). No polar hysteresis loop is observed. The solid line is a linear fit to the Kerr remanence above 1 ML thickness at 80 K. The nonzero intercept of the solid line at zero Co thickness is due to the spin polarization of Pt.

thickness range studied (0–5 ML), the film displays only a longitudinal hysteresis loop. This result is in contrast to the case of Co film grown on Pt(111), which displays a perpendicular magnetization in the ultrathin regime.²⁷ Figure 3 shows the magnetic remanence at 300 and 80 K as a function of the Co film thickness. At room temperature, the magnetic remanence starts to appear at ~ 1 ML Co thickness, increases quickly between 1 and 1.5 ML, and increases linearly above 1.5 ML thickness. The absence of the Kerr signal below 1 ML thickness implies that the Curie temperature of Co film below 1 ML is less than the room temperature. The SMOKE measurements at 80 K clearly show the existence of ferromagnetic orders in the submonolayer regime, as well as enhancement of the magnetic remanence above 1 ML thickness. The linear increase of the Kerr signal with film thickness above 1 ML simply reflects the additivity law for ultrathin ferromagnetic film.²³ The linear extrapolation of the Kerr signal (solid line in Fig. 3) gives a nonzero intercept of the Kerr signal at zero Co thickness. This result shows that Pt also contributes to the Kerr signal. This is not surprising because it is well known that a ferromagnetic layer induces spin polarization of adjacent Pt layer, and that the strong spin-orbit interaction of Pt and Pd could give rise a strong magneto-optic effect.^{28,29} Thus, the Co at the interface of Co/Pt(100) is expected to polarize the spins of Pt to make an additional contribution to the Kerr signal.

After annealing the film at 400 °C, the magnetic properties of the film change dramatically. The in-plane magnetization switches to out-of-plane below 2.5 ML thickness after annealing. The polar and longitudinal magnetic hysteresis loops are shown in Fig. 4. At about 2 ML thickness, the Co film possesses a clear polar hysteresis loop with full remanence, proving that the magnetization is perpendicular to the film plane. As the film thickness increases to 2.6 ML, the polar magnetic remanence decreases gradually, and meanwhile the longitudinal Kerr signal becomes observable. Above 2.8 ML, the polar signal decreases towards zero re-

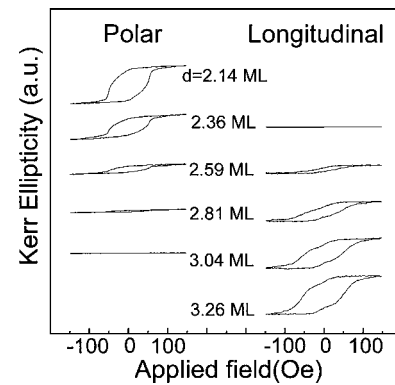


FIG. 4. Polar and longitudinal hysteresis loops of Co/Pt(100) film after annealing at 400 °C. Perpendicular magnetization is observed below 3 ML thickness.

manence and the longitudinal Kerr signal develops to a well defined hysteresis loop. The evolution of the magnetic hysteresis loop represents a spin reorientation transition (SRT) of the magnetization from perpendicular to parallel direction of the film plane.³⁰ The kinked shape of the longitudinal hysteresis loops suggests that there also exist interesting properties of the in-plane magnetic anisotropy. A detailed study is needed to understand the in-plane magnetic anisotropy, which is beyond the scope of this work. Figure 5 shows in detail the polar and longitudinal Kerr remanences as a function of the Co film thickness. Because the polar signal is much greater than the longitudinal signal, the polar signal has been scaled down in order to be displayed together with the longitudinal signal. The decrease of the polar Kerr signal below 2 ML is due to the suppression of the Curie temperature with decreasing film thickness. Figure 5 shows that the SRT thickness is ~ 2.7 ML, which is thinner than the Co/Pt(111) case, showing that the perpendicular magnetic anisotropy of the annealed Co/Pt(100) is weaker than that of Co/Pt(111). If we make an oversimplification that all the perpendicular magnetic anisotropy comes from the surface magnetic anisotropy, then we estimate that a magnitude of $2\pi M^2 d \sim 0.7$ erg/cm² of the surface anisotropy is needed to give a 2.7 ML SRT thickness.

It was shown that the SRT could occur by either a continuous rotation³¹ or by the formation of stripe magnetic domains.³² At present, it is unclear about by which of the two

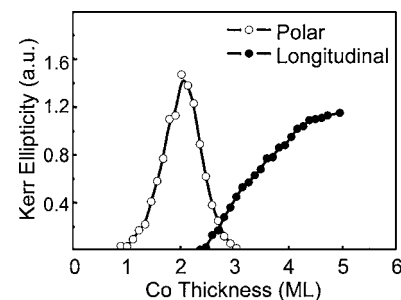


FIG. 5. Polar and longitudinal Kerr remanence versus the Co film thickness after annealing the Co/Pt(100) film at 400 °C. Spin reorientation transition occurs at ~ 2.7 ML.

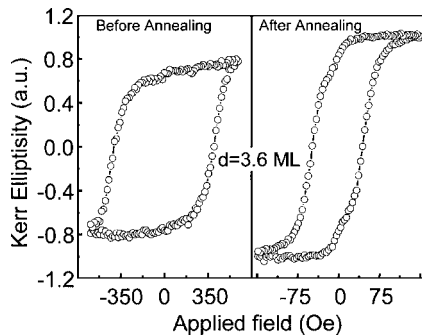


FIG. 6. Longitudinal hysteresis loops of Co(3.6 ML)/Pt(100) before and after annealing. Kerr signal enhancement after annealing is due to Co-Pt interfacial mixing.

ways the Co/Pt(100) SRT takes place. Microscopic magnetic domain imaging is needed to clarify the SRT nature. Above the SRT thickness, the longitudinal Kerr loop after annealing is also different as compared with Co film before annealing (Fig. 6). First, the magnitude of the Kerr signal is enhanced after annealing. For 3.6 ML film, the Kerr signal is enhanced by $\sim 25\%$ after annealing. This huge increase is unlikely due to the increased Co magnetic moment. Rather, we associate it with the increased number of spin-polarized Pt atoms due to the annealing. We previously mentioned that the STM measurement indicates that an annealing of the film promotes the Co-Pt intermixing to form a Co-Pt alloy layer at the Co/Pt interface. Therefore, the amount of Pt close to the ferromagnetic Co should increase after annealing. This is consistent with the SMOKE result that an annealing of the film increases the Kerr signal. The second observation is that the coercivity of the hysteresis loop is reduced. Since the coercivity is related to the domain wall pinning, the reduced coercivity is attributed to the smoothing of the film surface after annealing, as revealed by the STM measurement.

We now discuss the origin of the perpendicular magnetic anisotropy in the annealed Co/Pt(100) film. The existence of the perpendicular magnetization after annealing suggests that the perpendicular magnetic anisotropy is not from a sharp Co/Pt interface, but from the intermixed Co/Pt interface; i.e., from the Co-Pt interfacial alloy layer. Perpendicular magnetic anisotropy has been shown to be present in both epitaxially grown Co-Pt alloy films having a broad range of compositions³³ and in polycrystalline alloy films grown on amorphous substrates.³⁴ X-ray-absorption fine structure studies of Co-Pt alloy films suggest that the segregation of Co into monolayer-thick in-plane “platelets” or discontinuous “sheets” of Co is responsible for the perpendicular magnetic anisotropy.³⁴ This is consistent with our present work that an annealing of the film promotes the interfacial Co-Pt alloy formation and favors a perpendicular magnetic anisotropy. The interesting question is then if one monolayer Co-Pt interfacial alloy at the Co/Pt(100) interface is enough to result in the perpendicular magnetization. Photoemission experiment¹⁷ shows that the Co-Pt intermixing occurs even at room temperature. Thus, the Co-Pt alloy formation after annealing at 400 °C should extend more than 1 ML. Detailed knowledge of the interfacial properties of the

Co/Pt(100) relies on a detailed study of the Co-Pt alloy on Pt(100). This could be a project for future research.

IV. SUMMARY

In summary, Co ultrathin films are grown on Pt(100) and are investigated by LEED, STM, and SMOKE. Room-temperature-grown Co film shows in-plane magnetization. Annealing the film at 400 °C results in a perpendicular magnetic anisotropy, which leads to a SRT at ~ 2.7 ML thickness. We attribute the perpendicular magnetic anisotropy to the Co-Pt alloy formation at the Co/Pt(100) interface.

ACKNOWLEDGMENT

The work is supported by the Chinese National Science Foundation under Grant Nos. 60021403, 10134030, 60128404, Ministry of Science and Technology of China under Grant Nos. G001CB3095 and 2002CB613500, and by the US National Science Foundation DMR-0110034.

- ¹Y. P. Lee, R. Gontarz, and Y. V. Kudryavtsev, *Phys. Rev. B* **63**, 144402 (2001).
- ²J.-W. Lee, J. Kim, S.-K. Kim, J.-R. Jeong, and S.-C. Shin, *Phys. Rev. B* **65**, 144437 (2002).
- ³O. Rader, E. Vescovo, J. Redinger, S. Blügel, C. Carbone, W. Eberhardt, and W. Gudat, *Phys. Rev. Lett.* **72**, 2247 (1994).
- ⁴W. J. Antel Jr., M. M. Schwickert, T. Lin, W. L. O'Brien, and G. R. Harp, *Phys. Rev. B* **60**, 12933 (1999).
- ⁵C. L. Canedy, X. W. Li, and G. Xiao, *Phys. Rev. B* **62**, 508 (2000).
- ⁶S. Maat, K. Takano, S. S. P. Parkin, and E. E. Fullerton, *Phys. Rev. Lett.* **87**, 087202 (2001); T. L. Kirk, O. Hellwig, and E. E. Fullerton, *Phys. Rev. B* **65**, 224426 (2002).
- ⁷Z. Y. Liu and S. Adenwalla, *Phys. Rev. Lett.* **91**, 037207 (2003).
- ⁸B. N. Engel, C. D. England, R. A. Van Leeuwen, M. H. Wiedmann, and C. M. Falco, *Phys. Rev. Lett.* **67**, 1910 (1991).
- ⁹O. Robach, C. Quiros, P. Steadman, K. F. Peters, E. Lundgren, J. Alvarez, H. Isern, and S. Ferrer, *Phys. Rev. B* **65**, 054423 (2002).
- ¹⁰J.-W. Lee, J.-R. Jeong, S.-C. Shin, J. Kim, and S.-K. Kim, *Phys. Rev. B* **66**, 172409 (2002).
- ¹¹J. C. A. Huang, L. C. Wu, A. C. Hsu, Y. M. Hu, T. H. Wu, and C. H. Lee, *Phys. Rev. B* **59**, 1209 (1999).
- ¹²S.-B. Choe and S.-C. Shin, *Phys. Rev. Lett.* **86**, 532 (2001).
- ¹³S.-K. Kim and J. B. Kortright, *Phys. Rev. Lett.* **86**, 1347 (2001).
- ¹⁴D. Matsumura, T. Yokoyama, K. Amemiya, S. Kitagawa, and T. Ohta, *Phys. Rev. B* **66**, 024402 (2002).
- ¹⁵F. C. Chen, Y. E. Wu, C. W. Su, and C. S. Shern, *Phys. Rev. B* **66**, 184417 (2002).
- ¹⁶N. W. E. McGee, M. T. Johnson, J. J. de Vries, and J. van de Stegge, *J. Appl. Phys.* **73**, 3418 (1993).
- ¹⁷C. Boeglin, B. Carrière, J. P. Deville, F. Scheurer, C. Guillot, and N. Barrett, *Phys. Rev. B* **45**, 3834 (1992).
- ¹⁸C. H. Lee, R. F. C. Farrow, C. J. Lin, E. E. Marinero, and C. J. Chien, *Phys. Rev. B* **42**, 11384 (1990).
- ¹⁹C. Liu and S. D. Bader, *J. Appl. Phys.* **67**, 5758 (1990).
- ²⁰C. Liu and S. D. Bader, *Phys. Rev. B* **44**, 2205 (1991).
- ²¹X. F. Jin, J. Barthel, J. Shen, S. S. Manoharan, and J. Kirschner, *Phys. Rev. B* **60**, 11809 (1999).
- ²²P. Heilmann, K. Heinz, and K. Müller, *Surf. Sci.* **83**, 487 (1979).
- ²³Z. Q. Qiu and S. D. Bader, *J. Magn. Magn. Mater.* **200**, 664 (1999).
- ²⁴A. Borg, A.-M. Hilmen, and E. Bergene, *Surf. Sci.* **306**, 10 (1994).
- ²⁵P. van Beurden, B. S. Bunnik, G. J. Kramer, and A. Borg, *Phys. Rev. Lett.* **90**, 066106 (2003).
- ²⁶J. S. Tsay and C. S. Shern, *J. Appl. Phys.* **80**, 3777 (1996).
- ²⁷C. S. Shern, J. S. Tsay, H. Y. Her, Y. E. Wu, and R. H. Chen, *Surf. Sci.* **429**, L497 (1999).
- ²⁸W. Reim, H. Brändle, D. Weller, and J. Schoenes, *J. Magn. Magn. Mater.* **93**, 220 (1991).
- ²⁹H. J. Choi, R. K. Kawakami, E. J. Escorcia-Aparicio, Z. Q. Qiu, J. Pear-

- son, J. S. Jiang, D. Li, and S. D. Bader, *Phys. Rev. Lett.* **82**, 1947 (1999).
- ³⁰Z. Q. Qiu, J. Pearson, and S. D. Bader, *Phys. Rev. Lett.* **70**, 1006 (1993).
- ³¹M. Farle, B. Mirwald-Schulz, A. N. Anisimov, W. Platow, and K. Baberschke, *Phys. Rev. B* **55**, 3708 (1997).
- ³²R. Allenspach, M. Stampanoni, and A. Bischof, *Phys. Rev. Lett.* **65**, 3344 (1990).
- ³³S. Ferrer, J. Alvarez, E. Lundgren, X. Torrelles, P. Fajardo, and F. Boscherini, *Phys. Rev. B* **56**, 9848 (1997).
- ³⁴T. A. Tyson, S. D. Conradson, R. F. C. Farrow, and B. A. Jones, *Phys. Rev. B* **54**, R3702 (1996).